Search for the origin of wobbling motion in the $A \approx 130$ region: The case of ^{131}Xe

S. Chakraborty,[1,*] S. Bhattacharyya,[1,2,†] R. Banik,[3] Soumik Bhattacharya,[1,‡] G. Mukherjee,[1,2] C. Bhattacharya,[1,2] S. Biswas,[4,§] S. Rajbanshi,[5] Shabir Dar,[1,2] S. Nandi,[1,2,‖] Sajad Ali,[6] S. Chatterjee,[7] S. Das,[7] S. Das Gupta,[8] S. S. Ghugre,[7] A. Goswami,[9,2,¶] A. Lemasson,[4] Debasish Mondal,[1] S. Mukhopadhyay,[1,2] A. Navin,[4] H. Pai,[10] Surajit Pal,[1] Deepak Pandit,[1,2] R. Raut,[7] Prithwijita Ray,[11] M. Rejmund,[4] and S. Samanta[7,#]

[1]*Variable Energy Cyclotron Centre, Kolkata 700064, India*
[2]*Homi Bhabha National Institute, Mumbai 400094, India*
[3]*Institute of Engineering and Management, Kolkata 700091, India*
[4]*Grand Accélérateur National d'Ions Lourds (GANIL), CEA/DRF-CNRS/IN2P3, BP 55027, F-14076 Caen Cedex 5, France*
[5]*Department of Physics, Presidency University, Kolkata 700073, India*
[6]*Department of Physics, Government General Degree College at Pedong, Kalimpong 734311, India*
[7]*UGC-DAE Consortium for Scientific Research, Kolkata Centre, Kolkata 700098, India*
[8]*Department of Physics, Victoria Institution (College), Kolkata 700009, India*
[9]*Saha Institute of Nuclear Physics, Kolkata 700064, India*
[10]*Extreme Light Infrastructure - Nuclear Physics (ELI-NP), IFIN-HH, Bucharest-Magurele 077126, Romania*
[11]*Department of Physics, Acharya Brojendra Nath Seal College, Coochbehar 736101, India*

(Received 27 February 2023; revised 22 March 2023; accepted 19 May 2023; published 27 June 2023)

In-beam γ-ray spectroscopy of ^{131}Xe was carried out to study the structure of the intruder $\nu h_{11/2}$ band. Excited states were populated via an α-induced fusion-evaporation reaction at $E_\alpha = 38$ MeV. Inspection of $\gamma\gamma$-coincidence data resulted in the identification of a new rotational sequence. Based on the systematics of excitation energy, assigned spin-parity, decay pattern, and the electromagnetic character of the interband $\Delta I = 1$ γ transitions, this sequence is proposed as the unfavored signature partner of the $\nu h_{11/2}$ band. The structure of this band is further illuminated in the light of the triaxial particle rotor model (TPRM). The possibility of wobbling excitation in $N = 77$ Xe-Ba-Ce isotones was explored in a systematic manner.

DOI: 10.1103/PhysRevC.107.064318

I. INTRODUCTION

Rotational motion is a typical collective mode of excitation in atomic nuclei [1]. It originates to restore the rotational symmetry broken by nuclear deformation. The wave function of an axially symmetric (prolate or oblate) nucleus is invariant with respect to a rotation by an angle of 180° about an axis perpendicular to its symmetry axis ($\mathcal{R}$). The quantum number associated with the $\mathcal{R}$ operator is known as the signature (α) [2]. The even and odd spin sequences of a rotational band in even-A nuclei correspond to $\alpha = 0$, 1, respectively. Likewise, the $I = \frac{1}{2}, \frac{5}{2}, \frac{9}{2}, \ldots$ and $I = \frac{3}{2}, \frac{7}{2}, \frac{11}{2}, \ldots$ sequences in an odd-A nucleus correspond to $\alpha = \pm 1/2$. The signature-dependent splitting in energy is known as signature splitting $S(I)$ and can readily be extracted from the experimentally deduced level energies. The magnitude of $S(I)$ has a distinct K dependence (K is the projection of total angular momentum on the symmetry axis) [3]. For instance, in an axially symmetric nucleus, a rotational band with a high-K (low-K) configuration is predicted to exhibit a small (large) signature splitting [4]. However, in triaxially deformed nuclei, the quantity K no longer remains conserved and hence the band structures in these nuclei have mixed configurations of wave functions with different K values. As a consequence, a rotational phenomenon like signature splitting is found to appear in a different way than expected [5]. Thus, the quantity $S(I)$ was proposed to quantify the degree of triaxiality in atomic nuclei [6].

The rotational motion of a triaxially deformed nucleus can be realized by observing a pair of chiral doublet bands or a wobbling band or a γ band [2,7–9]. A large number of experimental signatures in favor of triaxial nuclear shapes have been found in the $A \approx 130$ region, mainly due to the presence of the unique parity shape driving $h_{11/2}$ orbital. Among these, the occurrence of wobbling bands at low angular momentum in normal-deformed γ-soft nuclei has drawn a lot of attention in the recent past. The rotational properties, such as moments

*saikat.c@vecc.gov.in
†sarmi@vecc.gov.in
‡Present address: Department of Physics, Florida State University, Tallahassee, Florida 32306, USA.
§Present address: Neutron and Muon Division, Paul Scherrer Institute, Forschungsstrasse 111, 5232 PSI-Villigen, Switzerland.
‖Present address: Physics Division, Argonne National Laboratory, Argonne, Illinois 60439, USA.
¶Deceased.
#Present address: Department of Physics, University of Genova, Via Dodecaneso 33, 16146 Genova, Italy.

of inertia, alignments, etc., and the decay pattern of these bands are quite similar to those of the unfavored signature partner band. But, the electromagnetic properties of the decay between favored and unfavoured signature partner bands were found to be different from the electromagnetic properties of the decay between two successive phonon wobbling bands. In the case of the signature partner band, the $\Delta I = 1$ transitions are primarily $M1$ in nature. On the other hand, such $\Delta I = 1$ γ rays between two consecutive phonon wobbling bands are expected to have a large $E2$ component. Thus, the structure of the $\alpha = +1/2$ partner of the intruder $h_{11/2}$ bands in odd-A triaxial nuclei has become a topic of current interest. In recent studies, based on the large δ value of the connecting $\Delta I = 1$ γ transitions, the so-called unfavored signature partner of the $\pi h_{11/2}$ bands in ^{135}Pr [10], ^{133}La [11] and the $\nu h_{11/2}$ bands in ^{133}Ba [12], ^{127}Xe [13], ^{105}Pd [14] have been reinterpreted in terms of wobbling excitation. In this context, it is also worth mentioning that in these nuclei (except in ^{133}La) apart from the wobbling band the unfavored signature partner band is also identified.

Since Xe isotopes are well known to have triaxial shapes [5], searching for the wobbling bands even in the heavier Xe nuclei would be promising. However, very recently most of these wobbling assignments were questioned from theoretical and/or experimental perspectives [15,16]. Hence, besides searching for the wobbling bands, proper identification of the unfavored signature partner band is essential to understand the nuclear structure of triaxial nuclei and to avoid any misinterpretation of the wobbling phenomenon. Among the more neutron-rich Xe isotopes, the experimental information on the low-lying yrast and non-yrast states in ^{131}Xe was extracted primarily from lighter-ion-induced fusion-evaporation reactions [17–20]. Later, the yrast negative parity band was extended up to $I^{\pi} = (35/2^{-})$ using two independent heavy-ion induced reactions [21]. However, only a limited spectroscopic information was reported on this nucleus from all of these studies. Recently, a detailed spectroscopic investigation of the high spin states in ^{131}Xe was carried out using an α-induced reaction, and that significantly extended the level scheme of this nucleus [22]. But, unlike the lighter Xe isotopes, the unfavored signature partner of the $\nu h_{11/2}$ band was not observed. As the odd quasineutron in this nucleus is expected to occupy the higher-Ω orbitals, the unfavored partner of the $\nu h_{11/2}$ band is expected to be observed. This is also evident from the recent observation of the unfavored partner of the $\nu h_{11/2}$ band in nthe $N = 77$ ^{133}Ba isotone [12]. Therefore, the aim of the present work is to search for the expected but heretofore unreported unfavored signature partner of the $\nu h_{11/2}$ band and/or wobbling band in $^{131}_{54}Xe_{77}$ from a reanalysis of the data reported in Ref. [22].

II. EXPERIMENTAL DETAILS

Excited states in ^{131}Xe were populated via the ^{130}Te(^{4}He, $3n\gamma$) fusion-evaporation reaction at $E_{\alpha} = 38$ MeV. An energetic beam of α particles was delivered by the K-130 cyclotron of the Variable Energy Cyclotron Centre (VECC), Kolkata, India [23]. An isotopically enriched target of ^{130}Te, evaporated on a 600 μg/cm^2 thick mylar backing, was 2 mg/cm^2 thick. Seven Compton-suppressed clover high-purity germanium (HPGe) detectors of the Indian National Gamma Array (INGA), arranged in three different angles $\theta = 40^{\circ}, 90^{\circ}, 125^{\circ}$ with respect to the beam direction, were employed to detect the deexciting γ rays [24]. A Pixie-16 (250 MHz, 12 bit, 16 channel) based digital data acquisition system was utilised to record the time-stamped valid events in single and coincident modes [25]. The gain-matched raw data were sorted to construct the symmetric and asymmetric matrices using the IUCPIX [25] data sorting package. Offline data analysis was carried out using INGASORT [26] and RADWARE [27] analysis packages. Further details of this experiment and the data analysis procedures are available in Refs. [22,28].

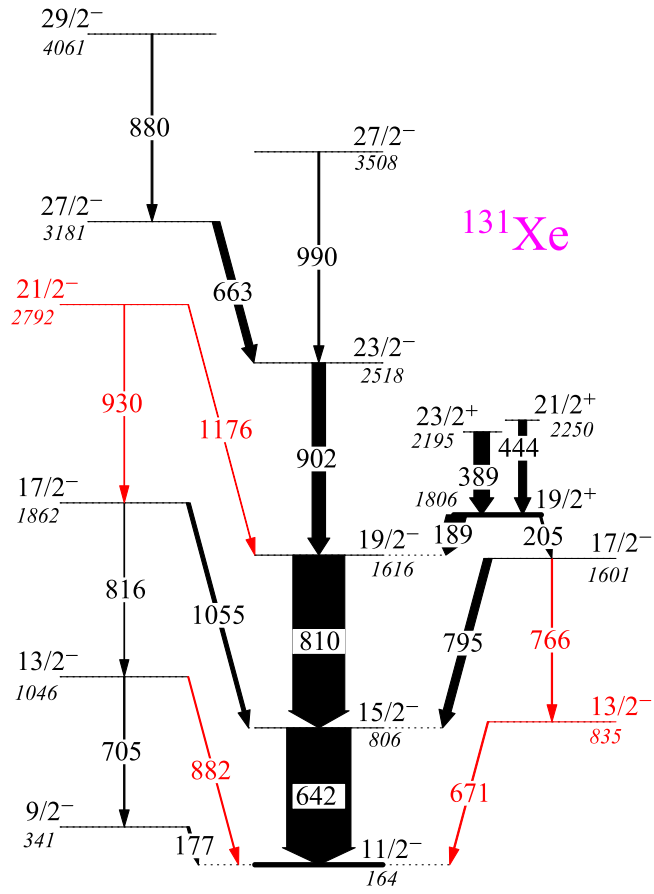

FIG. 1. Partial level scheme of ^{131}Xe, showing the negative parity levels and decaying γ rays of present interest. New experimental information is in red color.

III. RESULTS

From the present data analysis, a cascade of three γ transitions with $E_{\gamma} = 705$, 816, and 930 keV was established above the $I^{\pi} = 9/2^{-}$ state (Fig. 1). The levels of this sequence are also found to decay into the $\alpha = -1/2$ yrast negative parity levels through 177, 882, 1055, and 1176 keV γ rays. Pertinent energy gated γ spectra in favor of the new placements are shown in Fig. 2. In this work, the earlier reported 816 and 1055 keV γ transitions are found to be decaying

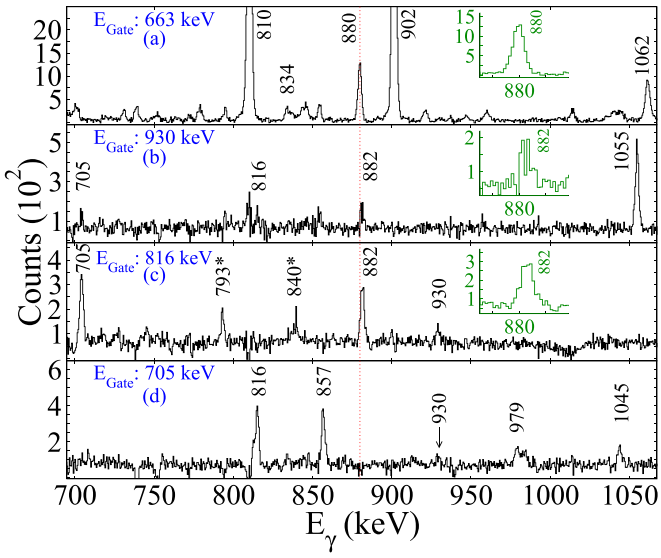

FIG. 2. Coincidence γ spectra, gated by (a) 663, (b) 930, (c) 816, and (d) 705 keV (top to bottom), to show the γ rays of present interest in ^{131}Xe. The γ rays which are marked here but not shown in the partial level scheme of ^{131}Xe are already reported in Ref. [22]. The asterisk ($*$) marked γ rays belong to ^{130}Te. The insets show the centroid difference of the 880 and 882 keV doublet transitions in the 663 and 816, 930 keV energy gates, respectively.

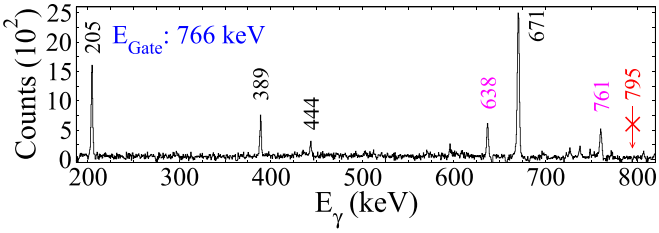

FIG. 3. Coincidence γ spectra, gated by 766 keV to show the γ rays of present interest in ^{131}Xe. The γ rays marked in magenta color are already placed in the positive parity band in this nucleus [22].

from the same $I^\pi = 17/2^-$ state at $E_{\rm level} = 1862$ keV [20,22]. Observation of both of these γ rays in the 930 keV energy gated spectrum [Fig. 2(b)] provides necessary support in favor of this assignment. The γ-ray peak that is observed at 881 keV in the total projection of the E_γ-E_γ matrix is found to be a doublet, composed of two transitions, of 880 and 882 keV. Thus, the placement of the 882 keV transition, in the presence of the 880 keV doublet, was difficult due to the lack of sufficient gating transitions. It shows a clear centroid difference between the peaks present in the 663 and 816 keV energy-gated spectra [see Figs. 2(a) and 2(c)]. Nonobservation of the 882 keV transition in the coincidence spectrum of the 705 keV gate provides further support in favor of its placement [Fig. 2(d)]. This sequence is extended further by placing an $E_\gamma = 930$ keV transition, based on its coincidence with the 705 and 816 keV γ rays (Fig. 2). However, the higher spin states of this band were not observed in the present work. Apart from these, two more γ rays, viz., $E_\gamma = 671$ and 766 keV, are also identified in this work. The $E_\gamma = 766$ keV transition is found to decay from the $I^\pi = 17/2^-$ state at $E_{\rm level} = 1601$ keV to a newly established state at $E_{\rm level} = 835$ keV (Fig. 1). This 835 keV state is observed to decay further to the isomeric $I^\pi = 11/2^-$ state at $E_{\rm level} = 164$ keV through the newly identified transition of $E_\gamma = 671$ keV (Fig. 1). The observation of the 671 keV transition and the absence of the 795 keV γ line in the 766 keV energy gated spectrum, as shown in Fig. 3, provide support for the placement of these new transitions.

To understand the origin of these newly observed sequences one needs to determine the multipole mixing ratio δ of the connecting γ transitions. The δ of a γ ray can be determined by comparing the experimentally measured angular distribution/correlation and/or linear polarization with their theoretical estimates. However, the linear polarization of weak transitions has large uncertainty and hence the angular correlation/distribution is used mainly to determine the multipole mixing ratio. In this work, the multipolarities of the observed γ rays are determined from the angular correlation ($R_{\rm DCO}$) measurement. Experimentally deduced $R_{\rm DCO}$ confirms the dipole character of the 671, 882, 1055, and 1176 keV γ rays and quadrupole character of the 705, 766, 816, and 930 keV γ rays, as listed in Table I. The $E2/M1$ multipole mixing ratios ($\delta_{E2/M1}$) of the interband $\Delta I = 1$ γ rays were estimated by comparing the experimental $R_{\rm DCO}$ with its theoretical values. The theoretical values of $R_{\rm DCO}$ for different δ were calculated using the computer code ANGCOR [29]. As a representative case, the variation of calculated DCO ratio,

TABLE I. Energies (E_γ and $E_{\rm level}$, in keV), relative intensities (I_γ), DCO ratios ($R_{\rm DCO}$, extracted from stretched $E2$ gates), linear polarization asymmetries ($\Delta_{\rm asym}$), and spin-parity (I^π) assignments for the γ rays/levels in ^{131}Xe.

(Uncertainty in E_γ is about 0.1–0.2 keV. The $E_{\rm level}$ are determined by fitting the measured energies of the γ rays shown in Fig. 1. The I_γ, $R_{\rm DCO}$, and Δ_{asym} of the known γ rays are adopted from Ref. [22].)

E_γ	$E_{\rm level}$	I_γ	$R_{\rm DCO}$	Δ_{asym}	$I_i^\pi \rightarrow I_f^\pi$
177.3	341.3	3.4 (2)	0.57 (2)		$9/2^- \rightarrow 11/2^-$
188.8	1805.6	3.1 (2)	0.82 (2)		$19/2^+ \rightarrow 19/2^-$
204.8	1805.6	<1	0.63 (2)		$19/2^+ \rightarrow 17/2^-$
389.0	2194.6	2.4 (1)	1.09 (2)	+0.08 (2)	$23/2^+ \rightarrow 19/2^+$
444.0	2249.5	1.2 (1)	0.61 (1)	−0.05 (3)	$21/2^+ \rightarrow 19/2^+$
642.3	806.0	100	1.01 (1)	+0.08 (1)	$15/2^- \rightarrow 11/2^-$
662.5	3180.9	11.7 (6)	0.97 (1)	+0.12 (2)	$27/2^- \rightarrow 23/2^-$
670.6	834.6	>1.8	0.57 (4)	−0.03 (5)	$13/2^- \rightarrow 11/2^-$
704.6	1046.0	2.0 (1)	1.28 (32)	+0.02 (1)	$13/2^- \rightarrow 9/2^-$
766.5	1600.9	≈ 1.8	1.15 (20)		$17/2^- \rightarrow 13/2^-$
794.8	1600.9	12.6 (2)	0.55 (1)	+0.03 (1)	$17/2^- \rightarrow 15/2^-$
810.5	1616.2	81 (4)	1.01 (1)	+0.10 (2)	$19/2^- \rightarrow 15/2^-$
815.6	1861.9	1.0 (1)	0.92 (7)	+0.03 (6)	$17/2^- \rightarrow 13/2^-$
880.1	4061.0	2.7 (1)	0.57 (3)	−0.10 (3)	$29/2^- \rightarrow 27/2^-$
881.8	1046.0	1.6 (1)	0.64 (11)		$13/2^- \rightarrow 11/2^-$
901.9	2517.8	21 (1)	1.01 (1)	+0.10 (1)	$23/2^- \rightarrow 19/2^-$
929.7	2792.1	<1	0.91 (24)		$21/2^- \rightarrow 17/2^-$
990.0	3508.2	2.8 (2)	0.94 (3)	+0.24 (3)	$27/2^- \rightarrow 23/2^-$
1055.1	1861.9	6.0 (2)	0.54 (3)	+0.02 (5)	$17/2^- \rightarrow 15/2^-$
1175.9	2792.1	≈ 1	0.64 (7)	−0.06 (9)	$21/2^- \rightarrow 19/2^-$

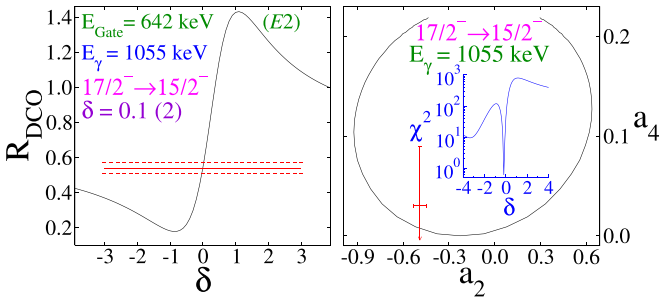

FIG. 4. Left: Variation of the theoretical DCO ratio as a function of multipole mixing ratio δ (black line). The solid (dashed) red lines indicate the experimentally measured $R_{\rm DCO}$ (error). Right: Contour plot of the angular distribution coefficients, a_2 vs a_4, for different δ (black line). Corresponding dispersion of experimental data, taken from Ref. [20], is marked with a red cross. The χ^2 analysis for the experimental distribution is shown in the inset (blue).

as a function of δ, is shown in the left panel of Fig. 4 for the 1055 keV ($17/2^- \rightarrow 15/2^-$) γ transition. The magnitude of $\delta_{1055\,\rm keV}$ is found to be approximately zero (Fig. 4) from the present analysis, which indicates almost pure $M1$ character of the 1055 keV γ ray. In an earlier experiment [20], the angular distribution coefficients [$a_2 = -0.49(4)$ and $a_4 = 0.03(6)$] of the 1055 keV γ ray were measured. The calculated a_2-a_4 contour plot, along with these experimentally measured values, is shown in the right panel of Fig. 4. The corresponding χ^2 analysis, as shown in the inset of the right panel of Fig. 4, also provides a low value of δ which is in good agreement with the δ value determined from the present angular correlation measurement. The similar magnitudes of $R_{\rm DCO} = 0.55(1)$, $a_2 = -0.47(3)$, and $a_4 = -0.03(8)$ are indicative of a similarly lower $\delta_{E2/M1}$ for the $E_\gamma = 795$ keV γ transition from $I_i^\pi = 17/2^-$ to $I_f^\pi = 15/2^-$ [17]. From a similar comparison of experimental and calculated DCO ratio as shown in Fig. 5, it is also evident that the magnitudes of δ of the two newly identified $\Delta I = 1$ γ transitions between $13/2^- \rightarrow 11/2^-$ states (i.e., $E_\gamma = 671$, 882 keV) are also very low ($\lesssim$0.1) and thus have very little $E2$ ($\approx$1%) admixture. In addition, the electric or magnetic nature of the γ transitions was determined from the linear polarization asymmetry (Δ_{asym}) measurement.

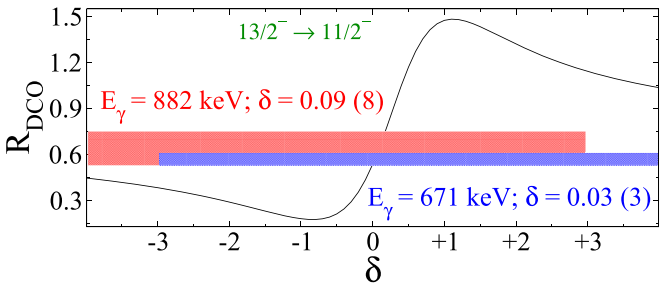

FIG. 5. Variation of the theoretical DCO ratio as a function of multipole mixing ratio δ (black line) for the $13/2^- \rightarrow 11/2^-$ transitions. The red (blue) shaded region corresponds to the experimental DCO ratio of the 882 (671) keV transition within the limits of uncertainty.

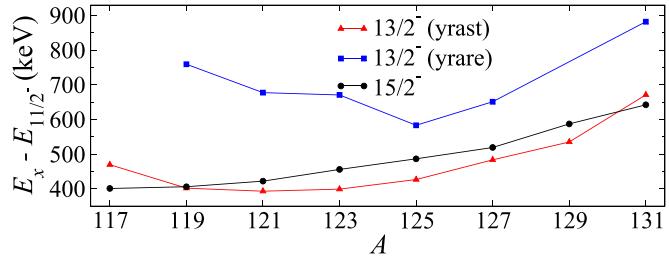

FIG. 6. Variation of the excitation energy of $15/2^-$ and $13/2^-$ (yrast and yrare) states, relative to the $E_{11/2^-}$, in $^{117-131}$Xe, as a function of mass number (A). Experimental data were taken from Refs. [13,22,30–35].

IV. DISCUSSION

The effect of intruder $h_{11/2}$ orbital, which gives an important piece of nuclear structural information in the proximity of $A \approx 125$ region, can be studied from the bands based on the $\nu h_{11/2}$ orbitals in Xe and Ba isotopes. Being associated with mid/high-Ω configurations, both the $\alpha = \pm 1/2$ signature partners of the $\nu h_{11/2}$ band were expected to be observed in these nuclei. Systematically, two $I^\pi = 13/2^-$ states were reported in $^{119-127}$Xe [13,31–34]. The excitation energies of these $I^\pi = 13/2^-$ and $I^\pi = 15/2^-$ states relative to the energy of $I^\pi = 11/2^-$ state (*i.e.*, E_x after subtracting $E_{11/2^-}$) are plotted as a function of mass number in Fig. 6 for all the Xe isotopes with $A = 117$–131. It is evident from this figure that the yrast (yrare) $13/2^-$ state in $^{119-127}$Xe is systematically found at a lower (higher) excitation energy than the $15/2^-$ state as shown in Fig. 6. In the case of ^{117,129}Xe, only the yrast $I^\pi = 13/2^-$ state was reported [30,35]. The rotational band built on the yrast $13/2^-$ states in $^{119-125}$Xe and ^{129}Xe was designated as the unfavored signature partner of the $\nu h_{11/2}$ band. On the other hand, the bands on yrare $13/2^-$ states in $^{119-125}$Xe were interpreted as the quasi-γ band coupled to the $h_{11/2}$ quasineutron (see [38] and references therein). However, these interpretations are not sufficient to justify the observed signature splitting in these bands, as discussed in Ref. [38]. Recent works on ^{127}Xe ($Z = 54$, $N = 73$) [13] and ^{133}Ba ($Z = 56$, $N = 77$) [12] reveal that the $13/2^-_{\rm yrast} \rightarrow 11/2^-$ γ transition is predominantly $E2$ ($\Delta I = 1$) in nature and, based on this, a different interpretation in terms of *wobbling motion* was proposed for the bands built on these states [12,13]. In contrast to this, the $13/2^-_{\rm yrare} \rightarrow 11/2^-$ γ transition is found to be primarily $M1$ in nature and hence the corresponding band is considered as the unfavored signature partner of the $\nu h_{11/2}$ band. However, unlike lighter $^{117-129}$Xe isotopes ($Z = 54$) and ^{133}Ba, ^{135}Ce isotones ($N = 77$), only the favored signature partner ($\alpha = +1/2$) of the $\nu h_{11/2}$ band was known from the previous studies on ^{131}Xe [21,22].

From the present study, both the yrast and yrare $I^\pi = 13/2^-$ states in ^{131}Xe are identified. But, in contrast to ^{127}Xe and ^{133}Ba, the $13/2^-_{\rm yrast} \rightarrow 11/2^-$ and $17/2^-_{\rm yrast} \rightarrow 15/2^-$ γ transitions in ^{131}Xe are found to be predominantly $M1$, thus excluding the possibility of wobbling nature of the sequence built on the yrast $I^\pi = 13/2^-$ state. To infer the structural evolution behind such a change, the properties, viz., 4^+ to

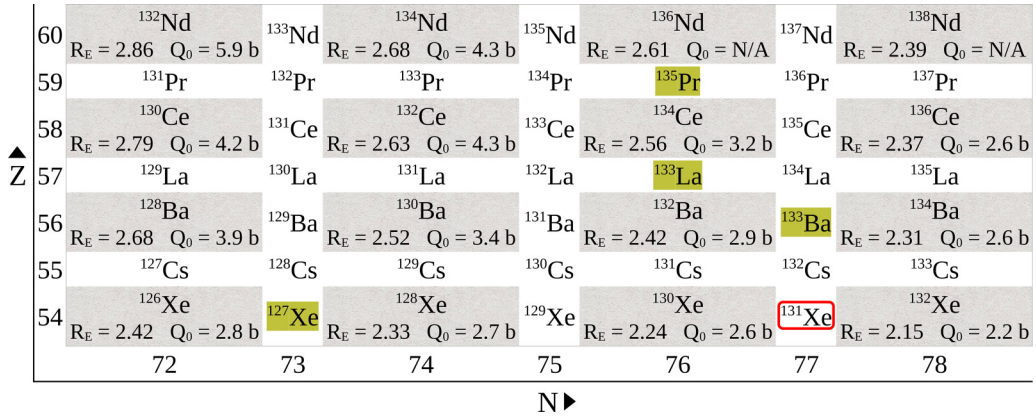

FIG. 7. A section of the Segrè chart showing the 4^+ to 2^+ energy ratio ($R_E = E_{4^+}/E_{2^+}$) and the intrinsic quadrupole moment (Q_0) of the *even-even* nuclei around $A \approx 130$ [36,37]. The highlighted odd-A nuclei are known for their wobbly nature [10–13]. The nucleus of present interest, ^{131}Xe, is marked with a red border.

2^+ energy ratio ($R_E = E_{4^+}/E_{2^+}$) and the intrinsic quadrupole moment (Q_0), of the even-even nuclei in this mass region were revisited. From this study it is found that the odd-A nuclei, where a wobbling band has been observed, are surrounded by two even-even nuclei with $R_E \geqslant 2.3$ and $Q_0 \geqslant 2.6$ b, as shown in Fig. 7. Also, two even-even nuclei, namely ^{130}Ba [39] and ^{136}Nd [40], having $R_E > 2.5$ are reported to exhibit a wobbling mode. From Casten's symmetry triangle it is known that the 4^+ to 2^+ energy ratio for γ-soft [O(6)] nuclei is found to be $R_E = 2.5$ [41]. However, the nucleus of current interest, ^{131}Xe, is surrounded by even-even ^{130,132}Xe nuclei with $R_E \approx 2.2$ and $Q_0 \leqslant 2.6$ b. With $R_E \approx 2.2$, the ^{130,132}Xe nuclei are found to be good candidates for the Z(4) model, thus indicating a transition from vibrator [U(5)] to γ-soft [O(6)] critical point symmetries [42]. Therefore, it perhaps can provide an information about the effect of R_E and/or Q_0 on the emergence of wobbling motion in atomic nuclei. However, the number of experimentally identified wobbling bands are quite limited, and more experimental investigations of the odd-A nuclei are required to understand the mechanism behind the appearance or disappearance of the wobbling mode in triaxial nuclei.

To check the above correlation between wobbling motion and R_E or Q_0, the available spectroscopic information on the ^{135}Ce was reinvestigated as a test case. The nucleus ^{135}Ce is of special interest as its neighbors show a variety of structural phenomena associated with the triaxial shapes of atomic nuclei. For instance, excitation of wobbling mode has been reported in ^{136,138}Nd [40,45], ^{135}Pr [10], ^{134}Ce [46], ^{133}La [11], and ^{133}Ba [12] nuclei. Another experimental fingerprint of nonaxial nuclear shapes is the observation of a pair of chiral doublet bands. Evidence of chiral doublet bands has been found in ^{135}Ce [47], as well as in several other neighboring nuclei such as $^{135-138}$Nd [45,48–51], ^{133}Ce [52], ^{133}La [53], and ^{131}Ba [54]. Apart from these, a number of γ-vibrational bands have been observed in this region. Recently, a new kind of excitation mode, namely, tilted precession (TiP), was also reported in ^{135}Nd [55]. The magnitudes of R_E and Q_0 of the neighboring even-even ^{134,136}Ce nuclei are found suitable to observe the wobbling excitation in triaxially deformed ^{135}Ce (Fig. 7). Figure 8 shows the negative parity bands in ^{131}Xe, ^{133}Ba, and ^{135}Ce associated with the $\nu h_{11/2}$ configuration. The sequence above the $I^\pi = 13/2^-$ state in ^{133}Ba is found to be due to the excitation of the wobbling mode [12]. Similarly to the case of ^{133}Ba, the magnitude of the DCO ratio of the connecting $\Delta I = 1$ transitions, e.g., $E_\gamma = 590$ and 724 keV, in ^{135}Ce are also found to be low compared to that expected for a pure dipole transition [43]. Also, the a_2 and/or a_4 angular distribution coefficients of these transitions are found to be higher than expected. These indicate a large $E2$ admixture in these γ rays and hence the band above the $I^\pi = 13/2^-$ state in ^{135}Ce is also found to be a possible candidate for a wobbling band. Detailed experimental fingerprints for this expected wobbling band in ^{135}Ce can be explored in a future experiment.

The spin-parity assignment and the decay pattern of the newly established band above the $I^\pi = 9/2^-$ state in ^{131}Xe make it a suitable candidate for the unfavored signature partner ($\alpha = -1/2$) of the $\nu h_{11/2}$ band. The multipole mixing ratio, estimated from the present spectroscopic results, indicates

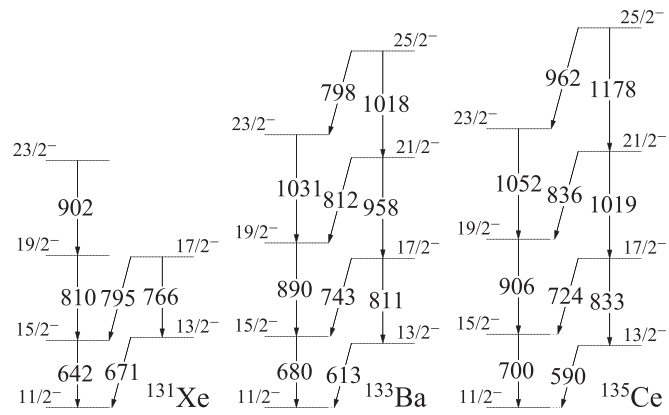

FIG. 8. Observed $\Delta I = 2$ bands on the yrast $I^\pi = 13/2^-$ states in ^{131}Xe (this work), ^{133}Ba [12], and ^{135}Ce [43] $N = 77$ isotones.

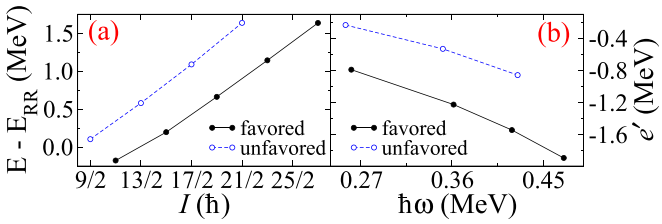

FIG. 9. Plots of (a) the observed level energies, after subtracting an average rigid-rotor energy, as a function of angular momentum and (b) the experimental Routhian as a function of rotational frequency for the $\nu h_{11/2}$ band in ^{131}Xe.

low $E2$ admixture in the $\Delta I = 1$ interband transitions. Such a low magnitude of δ is also found to be in agreement with this interpretation. The rotational properties such as the observed excitation energies relative to a rigid rotor ($E - E_{RR}$ [56]) and the experimental Routhian (e' [57]) are also found to exhibit similar character (Fig. 9) and hence providing further support in favor of the signature relationship of these bands.

The right panel of Fig. 10 shows the signature splitting, as a function of spin, of the $\alpha = \pm 1/2$ partners of the $\nu h_{11/2}$ band in ^{127}Xe [13], ^{131}Xe (this work), and ^{133}Ba [12]. The signature splitting [$S(I)$] of the $\nu h_{11/2}$ band in ^{131}Xe is found to be as large as that reported in ^{127}Xe and ^{133}Ba. Such an unexpectedly large $S(I)$ of the negative parity yrast levels was considered as a signature of γ deformation in ^{125}Xe [58]. Evidence of triaxial deformation in the form of wobbling motion was also reported in ^{127}Xe and ^{133}Ba [12,13]. Thus, ^{131}Xe may also possess a triaxial nuclear shape. Theoretical calculations successfully reproduced the $S(I)$ of the $\nu h_{11/2}$ band in several odd-A Xe-Ba isotopes [5]. Recently, a detailed theoretical investigation was carried out on $^{117-131}$Xe under the framework of the extended triaxial projected shell model (TPSM) [44]. This calculation is also able to reproduce the experimental $S(I)$ of ^{131}Xe quite successfully [Fig. 10(b)], but the calculated relative excitation energies of the states, i.e., $\Delta E_{\text{level}} \equiv E_\gamma$, in some cases differ from the corresponding experimental values. For instance, the magnitude of the $19/2^- \rightarrow 15/2^-$ ($23/2^- \rightarrow 19/2^-$) transition was smaller (larger) than expected (Fig. 11). In this work, a further theoretical investigation based on the triaxial particle rotor model

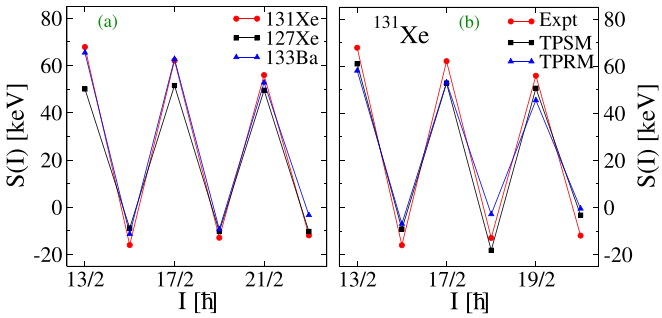

FIG. 10. (a) Left: Signature splitting of the $\alpha = \pm 1/2$ partners of the $\nu h_{11/2}$ band in ^{127}Xe [13], ^{131}Xe (this work), and ^{133}Ba [12]. (b) Right: Comparison of the experimental energy staggering between favored and unfavored signature partners of the $\nu h_{11/2}$ band with its theoretical estimates for ^{131}Xe.

(TPRM) was carried out to infer the microscopic structure of the negative parity band in ^{131}Xe.

Triaxial particle rotor model calculations

The triaxial particle rotor model is a widely used approach to study the spectroscopic features of low-lying states in the odd mass nuclei theoretically. Under this framework, an odd nucleon, located in a deformed single particle orbital, is supposed to rotate in the asymmetric potential of a triaxially deformed even-even core, characterized by the quadrupole deformation parameters (ϵ_2, γ). The Hamiltonian (H) of the coupled system is composed of the collective rotation of the even-even core (H_{core}), the single-particle Hamiltonian (H_{sp}), and the pairing interaction (H_{pair}). Thus, the total particle-rotor Hamiltonian can be expressed as

$$H = H_{\text{core}} + H_{sp} + H_{\text{pair}}.$$

The Hamiltonian of the rigid rotor can be written as

$$H_{\text{core}} = \sum_{k=1}^{3} A_k (I_k - j_k)^2,$$

where A_k are the hydrodynamical inertial parameters. The total angular momentum is expressed as I and the particle angular momentum as j. The single-particle Hamiltonian comprises a modified oscillator potential characterized by the deformation parameters: ϵ_2, ϵ_4 and γ. The pairing term is introduced via a standard BCS procedure to replace the single-particle energies by the quasiparticle energies. A complete description of this model is available in Refs. [59,60].

To start with, the input parameters reported in Ref. [5] are used to calculate the excitation energies of the negative parity states in ^{131}Xe. This nicely reproduces the favored partner, but underestimates the signature splitting (Fig. 11). The signature splitting, however, is found to be very sensitive to the triaxial deformation parameter γ, as was also demonstrated in the case of ^{125}Xe [58]. The relative excitation energy of the $I^\pi = 9/2^-$ state is also found to be different from its experimental value. Therefore, to achieve a good description of the experimental data, $\epsilon_2 = 0.13$ and $\gamma = 33^\circ$ deformation parameters were adopted finally [61]. The Coriolis attenuation factor $\xi = 1$ was used in this calculation [61]. These reproduce both favored and unfavored signature partners of the $\nu h_{11/2}$ band nicely, as shown in Fig. 11. The left panel of Fig. 10 shows a comparison of the experimental energy staggering between favored and unfavored signature partners of the $\nu h_{11/2}$ band with its theoretical estimates for ^{131}Xe. From the present investigation, it can be concluded that the ^{131}Xe nucleus has a triaxially deformed shape and the observed large signature splitting in negative parity band arises primarily due to this γ deformation.

To shed further light on the nature of the bands above the yrast and yrare $I^\pi = 13/2^-$ states, the ratio of the reduced magnetic dipole and electric quadrupole transition probabilities [$B(M1)/B(E2)$] was also estimated. The calculated $B(M1)/B(E2) = 1.27$ is found in good agreement with the experimentally determined $B(M1)/B(E2) = 1.27(14)$ for the yrare $I^\pi = 17/2^-$ state at $E_{\text{level}} = 1862$ keV. The multipole

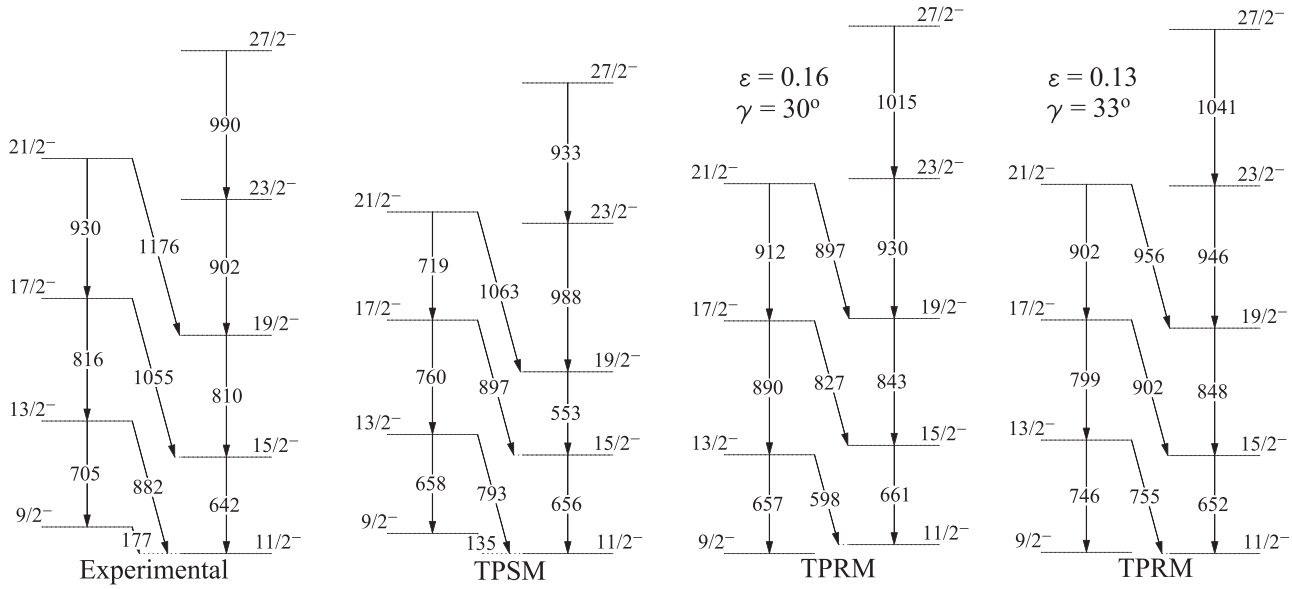

FIG. 11. A comparison of the experimental $\nu h_{11/2}$ band structure in ^{131}Xe with the theoretical predictions of the triaxial projected shell model (TPSM [44]) and triaxial particle rotor model (TPRM [5], present work).

mixing ratio, $\delta_{\mathrm{TPRM}} = -0.69$, of the corresponding $\Delta I = 1$ transition ($17/2^- \rightarrow 15/2^-$) is also found to be low. On the other hand, the experimental $B(M1)/B(E2) = 2.54(4)$ of the yrast $I^\pi = 17/2^-$ state is found to be two times higher in magnitude than that estimated from the TPRM calculation. Therefore, the band on the yrare $13/2^-$ state is considered as a more suitable candidate for the unfavored signature partner of the $\nu h_{11/2}$ band in ^{131}Xe. However, the origin of the yrast $13/2^-$ state still remains an open question and demands further investigations.

V. SUMMARY

In-beam γ ray spectroscopy of ^{131}Xe was carried out to study the structure of the intruder $\nu h_{11/2}$ band utilizing the Indian National Gamma Array. Excited states were populated via α induced fusion-evaporation reaction at $E_\alpha = 38$ MeV using the K-130 cyclotron of the Variable Energy Cyclotron Centre, Kolkata, India. Inspection of $\gamma\gamma$-coincidence data resulted in an identification of a rotational sequence which is found to decay into the yrast negative parity band. Based on the present spectroscopic results and the systematics of excitation energy, this sequence is proposed as the unfavored signature partner of the $\nu h_{11/2}$ band. The structure of this band is further investigated under the framework of the triaxial particle rotor model and the experimental outcomes are found to be in good agreement with theoretical estimates. Although the identification of the unfavored signature partner of the $\nu h_{11/2}$ band with a large signature splitting is a step forward towards the existence of the triaxial shape in this nucleus, no experimental signatures of the wobbling excitation were found in the present study. Thus, it can be concluded that the presence of triaxial deformation alone perhaps does not warrant an observation of wobbling motion in atomic nuclei.

ACKNOWLEDGMENTS

The authors are thankful to the INGA Collaboration, partially funded by Department of Science and Technology, Government of India, Project No. IR/S2/PF-03/2003-I, for making the detectors available and setting them up at VECC, Kolkata. Effort from the Accelerator group (VECC) personnel is thankfully acknowledged for providing a quality α beam during the experiment. Financial support of CEFIPRA/IFCPAR under Project No. 5604-4 is duly acknowledged. The first author (S.C.) sincerely acknowledges the financial support received from the Science and Engineering Research Board, Govt. of India (SERB, India) under the National Post-Doctoral Fellowship (N-PDF) scheme, Reference No. PDF/2022/001829.

[1] A. Bohr, Rev. Mod. Phys. **48**, 365 (1976).
[2] A. Bohr and B. R. Mottelson, *Nuclear Structure* (Benjamin, New York, 1975), Vol. II.
[3] F. Dönau, Nucl. Phys. A **471**, 469 (1987).
[4] Y. Liang, R. Ma, E. S. Paul, N. Xu, D. B. Fossan, J.-Y. Zhang, and F. Donau, Phys. Rev. Lett. **64**, 29 (1990).
[5] A. Gelberg, D. Lieberz, P. von Brentano, I. Ragnarsson, P. B. Semmes, and I. Wiedenhöver, Nucl. Phys. A **557**, 439 (1993).
[6] M. W. Reed *et al.*, Phys. Lett. B **752**, 311 (2016).
[7] S. Frauendorf and J. Meng, Nucl. Phys. A **617**, 131 (1997).
[8] S. Frauendorf and F. Dönau, Phys. Rev. C **89**, 014322 (2014).
[9] A. S. Davydov and G. F. Filippov, J. Exp. Theor. Phys. **35**, 440 (1958).
[10] J. T. Matta *et al.*, Phys. Rev. Lett. **114**, 082501 (2015).
[11] S. Biswas *et al.*, Eur. Phys. J. A **55**, 159 (2019).

[12] K. Rojeeta Devi *et al.*, Phys. Lett. B **823**, 136756 (2021).
[13] S. Chakraborty *et al.*, Phys. Lett. B **811**, 135854 (2020).
[14] J. Timár *et al.*, Phys. Rev. Lett. **122**, 062501 (2019).
[15] K. Nomura and C. M. Petrache, Phys. Rev. C **105**, 024320 (2022).
[16] B. F. Lv *et al.*, Phys. Lett. B **824**, 136840 (2022).
[17] A. Kerek, A. Luukko, M. Grecescu, and J. Sztarkier, Nucl. Phys. A **172**, 603 (1971).
[18] D. C. Palmer, A. D. Irving, P. D. Forsyth, I. Hall, D. G. E. Martin, and M. J. Maynard, J. Phys. G: Nucl. Phys. **4**, 1143 (1978).
[19] A. D. Irving, P. D. Forsyth, I. Hall, and D. G. E. Martin, J. Phys. G: Nucl. Phys. **5**, 1595 (1979).
[20] T. Lönnroth, J. Kumpulainen, and C. Tuokko, Phys. Scr. **27**, 228 (1983).
[21] L. Kaya *et al.*, Phys. Rev. C **98**, 014309 (2018).
[22] R. Banik *et al.*, Phys. Rev. C **101**, 044306 (2020).
[23] S. Bhattacharya, C. Bhattacharya, P. Das, G. Mukherjee, and T. K. Ghosh, Eur. Phys. J. A **54**, 158 (2018).
[24] S. Bhattacharya *et al.*, Proc. DAE Symp. Nucl. Phys. **63**, 1156 (2018).
[25] S. Das *et al.*, Nucl. Instrum. Methods Phys. Res. Sect. A **893**, 138 (2018).
[26] R. Bhowmik, S. Muralithar, and R. P. Singh, Proc. DAE Symp. Nucl. Phys. **44B**, 422 (2001).
[27] D. C. Radford, Nucl. Instrum. Methods Phys. Res. Sect. A **361**, 297 (1995).
[28] R. Banik, Single Particle and Collective Excitations near Z=50, Ph.D. thesis, Homi Bhabha National Institute, Mumbai, India, 2020 (unpublished).
[29] E. S. Macias, W. D. Ruhter, D. C. Camp, and R. G. Lanier, Comput. Phys. Commun. **11**, 75 (1976).
[30] Z. Liu *et al.*, Eur. Phys. J. A **1**, 125 (1998).
[31] C.-B. Moon, T. Komatsubara, Y. Sasaki, T. Jumatsu, K. Yamada, K. Satou, and K. Furuno, Eur. Phys. J. A **14**, 13 (2002).
[32] J. Timár, J. Simpson, E. S. Paul, S. Araddad, C. W. Beausang, M. A. Bentley, M. J. Joyce, and J. F. Sharpey-Schafer, J. Phys. G **21**, 783 (1995).
[33] A. Basu *et al.*, Phys. Rev. C **101**, 024309 (2020).
[34] A. Al-Khatib *et al.*, Phys. Rev. C **83**, 024306 (2011).
[35] Y. Huang *et al.*, Phys. Rev. C **93**, 064315 (2016).
[36] National Nuclear Data Center, Brookhaven National Laboratory, Upton, New York 11973-5000, USA.
[37] S. Raman, C. W. Nestor, and P. Tikkanen, At. Data Nucl. Data Tables **78**, 1 (2001).
[38] C. B. Moon, C. S. Lee, T. Komatsubara, Y. Sasaki, and K. Furuno, Phys. Rev. C **76**, 067301 (2007).
[39] Q. B. Chen, S. Frauendorf, and C. M. Petrache, Phys. Rev. C **100**, 061301(R) (2019).
[40] B. F. Lv *et al.*, Phys. Rev. C **105**, 034302 (2022).
[41] R. F. Casten, Nat. Phys. **2**, 811 (2006).
[42] D. Bonatsos, D. Lenis, D. Petrellis, P. A. Terziev, and I. Yigitoglu, Phys. Lett. B **621**, 102 (2005).
[43] R. Ma, E. S. Paul, D. B. Fossan, Y. Liang, N. Xu, R. Wadsworth, I. Jenkins, and P. J. Nolan, Phys. Rev. C **41**, 2624 (1990).
[44] S. Jehangir, N. Nazir, G. H. Bhat, J. A. Sheikh, N. Rather, S. Chakraborty, and R. Palit, Phys. Rev. C **105**, 054310 (2022).
[45] C. M. Petrache *et al.*, Phys. Rev. C **86**, 044321 (2012).
[46] C. M. Petrache and S. Guo, arXiv:1603.08247.
[47] H. C. Jain, S. Lakshmi, and P. K. Joshi, AIP Conf. Proc. **764**, 99 (2005).
[48] S. Zhu *et al.*, Phys. Rev. Lett. **91**, 132501 (2003).
[49] S. Mukhopadhyay *et al.*, Phys. Rev. Lett. **99**, 172501 (2007).
[50] C. M. Petrache *et al.*, Phys. Rev. C **97**, 041304(R) (2018).
[51] C. M. Petrache *et al.*, Eur. Phys. J. A **56**, 208 (2020).
[52] A. D. Ayangeakaa *et al.*, Phys. Rev. Lett. **110**, 172504 (2013).
[53] C. M. Petrache *et al.*, Phys. Rev. C **94**, 064309 (2016).
[54] S. Guo *et al.*, Phys. Lett. B **807**, 135572 (2020).
[55] B. F. Lv *et al.*, Phys. Rev. C **103**, 044308 (2021).
[56] I. Ragnarsson, Z. Xing, T. Bengtsson, and M. A. Riley, Phys. Scr. **34**, 651 (1986).
[57] R. Bengtsson and S. Frauendorf, Nucl. Phys. A **314**, 27 (1979).
[58] D. Lieberz, A. Gelberg, P. von Brentano, I. Ragnarsson, and P. B. Semmes, Phys. Lett. B **282**, 7 (1992).
[59] S. E. Larsson, Phys. Scr. **8**, 17 (1973).
[60] S. E. Larsson, G. Leander, and I. Ragnarsson, Nucl. Phys. A **307**, 189 (1978).
[61] S. Chakraborty and S. Bhattacharyya, Proc. DAE Symp. Nucl. Phys. **66**, 106 (2022).